Contribution from the Department of Chemistry,
Purdue University, West Lafayette, Indiana 47907

Solution Properties of Bis(dipeptide)nickelate(III) Complexes and Kinetics of Their Decomposition in Acid

STEPHEN A. JACOBS and DALE W. MARGERUM*

Received August 8, 1983

Oxidation of blue bis(dipeptide)nickelate(II) complexes yields violet-black solutions of nickel(III) complexes, which are long-lived species in neutral solution. Dipeptides with glycyl, alanyl, and α-aminoisobutyryl residues are examined. The electron paramagnetic resonance spectra of frozen aqueous glasses have $g_{\parallel}$ greater than $g_{\perp}$ for the nickel(III) complexes. The unpaired electron appears to be in the $d_{x^2-y^2}$ orbital of a tetragonally compressed octahedral environment, in contrast to its presence in the d_{z^2} orbital in the tetragonally elongated octahedral geometry found for many other nickel(III) complexes. Acid catalyzes the rearrangement of the violet-black species to a yellow nickel(III) complex, which has properties more typical of other nickel(III) peptide species. This reaction is not reversible. Below pH 2 sequential reactions are observed with an acid-catalyzed conversion of the violet-black to the yellow complex, followed by an acid-independent decomposition of the yellow nickel(III) complex to nickel(II). The first step is first order in $[H^+]$ and in [Ni(III)] with rate constants (25.0 °C) that vary from 5.6 to 160 M^{-1} s^{-1} for different dipeptides. The rate constants for the second step also vary with the dipeptide and range from 0.016 to 0.15 s^{-1}. Above pH 3 the intermediate yellow species does not form in appreciable concentrations.

Introduction

Recently the less common trivalent oxidation state has been invoked to explain paramagnetic centers in several nickel-containing systems of biological interest.[1-5] Nickel(III) deprotonated peptide complexes are readily obtained from the corresponding nickel(II) complexes by chemical or electrochemical oxidation,[6] and the properties of trivalent nickel can be studied.

Investigations of nickel(III) oligopeptide complexes by electron paramagnetic resonance,[7-10] electrochemistry,[8,10-13] circular dichroism,[14] and chemical reactivity[8,13,15-17] have revealed detailed information about their structural and chemical properties in aqueous solution. Although these investigations have been directed primarly toward the 1:1 complexes, a bis complex $[Ni^{III}(H_{-2}G_3a)(H_{-1}G_3a)]$ (where G_3a is triglycinamide and H_{-n} refers to n deprotonated peptide nitrogens coordinated to the metal) has been proposed on the basis of EPR evidence.[7] Recently, the bis(triglycine) complex of nickel(III) has been found to exist in two forms.[16,18] Frozen EPR as well as room-temperature EPR and UV–visible spectra support the stepwise formation of two different bis(tripeptide) complexes as a function of pH, formed from the nickel(III) mono complex with excess ligand.

Nickel(II) in the presence of excess glycylglycine forms a blue complex[19-21] whose structure has been determined by single-crystal, X-ray diffraction.[22,23] The metal is surrounded by two mutually perpendicular glycylglycine residues that act as tridentate ligands *via* their amino, deprotonated peptide, and carboxyl groups. The Ni–N(deprotonated peptide) bonds (1.99 Å) are shorter than the Ni–O(carboxyl) bonds (2.17 Å) and Ni–N(amino) bonds (2.14 Å). This places the nickel(II) in a compressed octahedral environment. This coordination geometry with high-spin nickel(II) is unusual for peptide complexes of nickel(II), which tend to form low-spin square-planar complexes.[19,20] The two amine and two deprotonated peptide nitrogen coordinated to the nickel(II) in the bis complex provide a suitable environment to stabilize nickel(III).[11]

In the present study the solution properties of the violet-black bis(dipeptide)nickelate(III) complexes of glycylglycine, L-alanylglycine, L-alanyl-L-alanine, glycyl-L-alanine, and α-aminoisobutyrylglycine are characterized. Investigation of the kinetics and a proposed mechanism of their acid-catalyzed decomposition reactions are reported.

Experimental Section

Reagents. Chromatographically pure dipeptides glycylglycine (GlyGly, Sigma Chemical Co.), L-alanylglycine (AlaGly, Schwarz/Mann), L-alanyl-L-alanine (AlaAla, Biosynthetika), and glycyl-L-alanine (GlyAla, Biosynthetika) were used as supplied. The dipeptide AibGly with the amino acid residue α-aminoisobutyric acid (Aib) was synthesized according to procedures reported elsewhere.[24] Anal. Calcd for $C_6H_{12}N_2O_3$: C, 44.99; H, 7.55; N, 17.49. Found: C, 45.22; H, 7.48; N, 17.21. A stock solution of $Ni(ClO_4)_2$ was prepared by the reaction of $NiCO_3$ and $HClO_4$ and was standardized against EDTA with murexide indicator.

Solutions of the bis(dipeptide)nickelate(II) complexes were prepared by the reaction of 3 equiv of the ligand with $Ni(ClO_4)_2$. Upon slow addition of NaOH the green solution turned light blue, at pH 11, with the formation of the fully deprotonated bis complex.[19-21,23] The complex was electrochemically oxidized in a flow system. The electrode arrangement had a graphite-powder working electrode packed in a porous Vycor glass column wrapped externally with a platinum-wire

(1) Lancaster, J. R. *Science (Washington, D.C)* **1982**, *216*, 1324–1325.
(2) Cammack, R.; Patil, D.; Aguirre, R.; Hatchikian, E. C. *FEBS Lett.* **1982**, *142*, 289–292.
(3) LaGall, J.; Ljungdahl, P. O.; Moura, I.; Peck, H. D.; Xavier, A. V.; Moura, J. J.; Teixera, M.; Huynh, B. H.; DerVartanian, D. V. *Biochem. Biophys. Res. Commun.* **1982**, *106*, 610–616.
(4) Albracht, S. P. J.; Graf, E. G.; Thauer, R. K. *FEBS Lett.* **1982**, *140*, 311–313.
(5) Lancaster, J. R. *FEBS Lett.* **1980**, *115*, 285–288.
(6) Bossu, F. P.; Margerum, D. W. *J. Am. Chem. Soc.* **1976**, *98*, 4003–4004.
(7) Lappin, A. G.; Murray, C. K.; Margerum, D. W. *Inorg. Chem.* **1978**, *17*, 1630–1634.
(8) Murray, C. K.; Margerum, D. W. *Inorg. Chem.* **1982**, *21*, 3501–3506.
(9) Sugiura, Y.; Mino, Y. *Inorg. Chem.* **1979**, *18*, 1336–1339.
(10) Sakurai, T.; Hongo, J.; Nakahara, A.; Nakao, Y. *Inorg. Chim. Acta* **1980**, *46*, 205–210.
(11) Bossu, F. P.; Margerum, D. W. *Inorg. Chem.* **1977**, *16*, 1210–1214.
(12) Youngblood, M. P.; Margerum, D. W. *Inorg. Chem.* **1980**, *19*, 3068–3072.
(13) Murray, C. K.; Margerum, D. W. *Inorg. Chem.* **1983**, *22*, 463–469.
(14) Czarnecki, J. J.; Margerum, D. W. *Inorg. Chem.* **1977**, *16*, 1997–2003.
(15) Bossu, F. P.; Paniago, E. B.; Margerum, D. W.; Kirksey, S. T., Jr.; Kurtz, J. L. *Inorg. Chem.* **1978**, *17*, 1034–1042.
(16) Margerum, D. W. *Pure Appl. Chem.* **1983**, *55*, 23–34.
(17) Margerum, D. W. *Adv. Chem. Ser.* **1982**, *No. 198*, 3–38.
(18) Kirvan, G. E.; Margerum, D. W., to be submitted for publication.
(19) Martin, R. B.; Chamberline, M.; Edsall, J. T. *J. Am. Chem. Soc.* **1960**, *82*, 495–498.
(20) Kim, M. K.; Martell; A. E. *J. Am. Chem. Soc.* **1967**, *89*, 5138–5144.
(21) Nag, K.; Banerjee, P. *J. Inorg. Nucl. Chem.* **1975**, *37*, 1521–1525.
(22) Freeman, H. C.; Guss, J. M.; Sinclair, R. L. *Chem. Commun.* **1968**, 485–487.
(23) Freeman, H. C.; Sinclair, R. L. *Acta Crystallogr., Sect. B* **1978**, *B34*, 2451–2458.
(24) Kirksey, S. T., Jr.; Neubecker, T. A.; Margerum, D. W. *J. Am. Chem. Soc.* **1979**, *101*, 1631–1633.

0020-1669/84/1323-1195$01.50/0

auxiliary electrode.[25] Millimolar solutions of the bis(dipeptide)-nickelate(II) complexes were oxidized at 850 mV vs. Ag/AgCl at a flow rate of 1 mL/min. The resulting violet-black solutions were collected unbuffered (pH ca. 7.5) and were stable for several days at room temperature.

Measurements. Electron paramagnetic resonance spectra of magnetically dilute aqueous glasses containing the nickel(III) complexes (ca. 10^{-4} M) were measured with a Varian E-109 X-band spectrometer modulated at 100 kHz. The EPR was equipped with the Varian E-231 variable-temperature cavity and a Varian E-238 variable-temperature controller. Samples were quenched rapidly in liquid nitrogen, and the temperature was maintained at -150 ± 5 °C. Magnetic field values were measured relative to α,α'-diphenyl-β-picrylhydrazyl ($g = 2.004$). Spectroscopic splitting factors (g values) and hyperfine coupling constants (a values) were determined by generating the "best-fit" curves using a computer spectrum matching procedure.[26]

Room-temperature EPR spectra were obtained on a Varian E-231 multipurpose cavity with a thin (0.1 mm) quartz cell that was equipped with a two-jet tangential mixer. Dynamic measurements used a Varian E-271A rapid-scan unit that was interfaced to an 8080A based microcomputer, a controller/function generator combination, and the Varian E-109 spectrometer. In this configuration small changes in the bulk magnetic field were generated linearly with time. EPR spectra with this stopped-flow system could be generated with spectral windows of 0.1–100 G in time intervals as short as 30 ms.[27]

A Vidicon rapid-scanning stopped-flow spectrometer[28,29] or a HP 8450A spectrometer was used to obtain UV–visible spectra of short-lived nickel(III) species in acid (pH <2.5). The HP 8450A was used in the two-step, three-reagent mixing experiments, which were performed to test the chemical reversibility of the acid-catalyzed decomposition reactions.

The photochemical apparatus and methodology is described elsewhere.[30] The nickel(II) solution (pH 7.6, $I = 1.0$ ($NaClO_4$)) was bubbled with argon to purge oxygen. The nickel(III) complex was assayed spectrophotometrically prior to and after photolysis (11-min exposure in a 1-cm cell at 25 °C).

Above pH 2 the hydrogen ion concentration was determined with an Orion Model 601A research pH meter equipped with a Corning 4760S1 combination electrode or with a Radiometer Model PHM26 research pH meter equipped with micro Radiometer glass (Model G222B) and calomel (Model K4112) electrodes. Perchloric acid–sodium hydroxide titrations in 0.1 and in 1.0 M $NaClO_4$ were used to calibrate the electrodes.

Kinetics of the nickel(III) decomposition reactions were measured under pseudo-first-order conditions (constant pH) with the nickel(III) complex as the limiting reagent. Absorbance vs. time profiles were generated by using a Cary 16 or a Durrum stopped-flow spectrometer.[31]

Results and Discussion

Nickel(II) forms a blue complex with two molecules of dipeptide, and for the case of glycylglycine the geometry has been shown to be a tetragonally compressed octahedron.[22,23] Electrochemical or chemical oxidation of the nickel(II) species results in the formation of a violet-black paramagnetic complex with the proposed formula $Ni^{III}(H_{-1}GlyGly)_2^-$. This complex lasts for several days in neutral solution at room temperature. Upon addition of acid (pH <2), a transient yellow species is generated. This short-lived complex is also paramagnetic and has properties similar to those of nickel(III) peptide complexes that have a tetragonally elongated geometry.[11] The yellow intermediate undergoes a self-redox reaction to give colorless diamagnetic products.

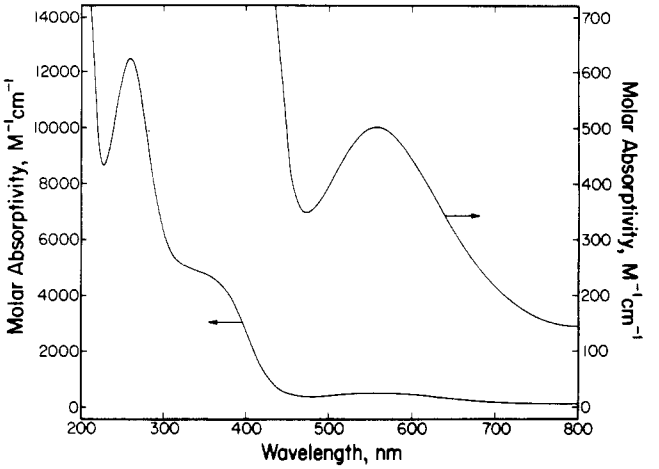

Figure 1. UV–visible spectrum of the violet-black $Ni^{III}(H_{-1}GlyGly)_2^-$ complex.

Violet-Black Nickel(III) Species. Oxidation of the $Ni^{II}(H_{-1}GlyGly)_2^{2-}$ complex causes a change in the electronic absorption bands from 366 and 610 to 255, 355 (sh), and 560 nm as shown in Figure 1. The molar absorptivity at 560 nm is 500 ± 30 as determined by a redox titration of the trivalent nickel complex with ascorbic acid. The dipeptides AlaGly, AibGly, GlyAla, and AlaAla all yield complexes with similar spectral properties. This type of similarity is not unusual as the spectral properties of 19 bis(dipeptide)cobaltate(III) complexes have been reported[32] in which the average λ_{max} was 523 ± 3 nm and the average molar absorptivity was 390 ± 20 M^{-1} cm^{-1}.

Photochemical Redox. The redox decomposition of $Ni^{III}(H_{-1}AlaGly)_2^-$ (2.6×10^{-4} M initially) is photochemically catalyzed. The quantum yield for loss of nickel(III) at 280 nm (ϕ_{280}) is 0.03. Although this value is much lower than that found for $Ni^{III}(H_{-2}Aib_3)$[33] ($\phi_{280} = 0.21$), the photochemical reaction is a significant decomposition pathway.

Redox Potential. The violet-black $Ni^{III}(H_{-1}GlyGly)_2^-$ complex readily oxidizes I^- ($E^{\circ\prime} = 0.62$ V) and $Cu^{II}(H_{-2}Aib_3)^-$ ($E^{\circ\prime} = 0.66$ V). $Ni^{III}(H_{-1}GlyGly)_2^-$ does not react with $Ni^{II}(H_{-2}G_3)^-$, ($E^{\circ\prime} = 0.85$ V) or with $Ni^{II}(H_{-2}Aib_3)^-$ ($E^{\circ\prime} = 0.83$ V). Aqueous bromine ($E^{\circ\prime} \cong 1$ V) and OXONE ($KHSO_5$, $E^{\circ\prime} \cong 1.4$ V) oxidize the Ni(II) to Ni(III). Attempts to obtain the reduction potentials using cyclic voltammetry or differential-pulse voltammetry at glassy-carbon and other electrodes were unsuccessful because of poor reversibility. The reduction potential ($E^{\circ\prime}$) of the $Ni^{III,II}(H_{-1}GlyGly)_2^{-,2-}$ complex is estimated to be between 0.66 and 0.83 V (vs. NHE). This is within the range estimated by Meyerstein for $Ni^{III,II}EDTA$ ($0.54 \leq E^{\circ\prime} \leq 1.06$ V).[34]

EPR Spectra. In previous EPR studies of nickel(III) peptides[7-10] an axially elongated tetragonal distortion was found with $g_{xx}, g_{yy} > g_{zz}$. The hyperfine splitting from equatorially bound nitrogens could not be resolved, and broadening parameters ($W_{xx}, W_{yy} > W_{zz}$) were used to match the calculated and observed spectra.[7] However, axially coordinated nitrogens caused readily observable hyperfine splitting because the unpaired electron was in the d_{z^2} orbital. These spectra were calculated with values[7] of 19–24 G for the hyperfine coupling constants, a_{zz}.

The frozen EPR spectrum for $Ni^{III}(H_{-1}GlyGly)_2^-$, given in Figure 2, corresponds to that of a nonaxially symmetric complex with one unpaired electron. The average g value (g_{av} =

(25) Clark, B. R.; Evans, D. H. *J. Electroanal. Chem.* **1965**, *69*, *181*–194.
(26) Toy, A. D.; Chaston, S. H. H.; Pilbrow, J. R.; Smith, T. D. *Inorg. Chem.* **1971**, *10*, 2219–2226.
(27) Jacobs, S. A., Ph.D. Thesis, Purdue University, 1983.
(28) Ridder, G. M.; Margerum, D. W. *Anal. Chem.* **1977**, *49*, 2098–2108.
(29) Milano, M. J.; Pardue, H. L.; Cook, T.; Santini, R. E.; Margerum, D. W.; Raycheba, J. M. T. *Anal. Chem.* **1974**, *46*, 374–381.
(30) Hamburg, A. W.; Margerum, D. W. *Inorg. Chem.* **1983**, *22*, 3884–3893.
(31) Willis, B. G.; Bittikofer, J. A.; Pardue, H. L.; Margerum, D. W. *Anal. Chem.* **1970**, *42*, 1340–1349.
(32) Boas, L. V.; Evans, C. A.; Gillard, R. D.; Mitchell, P. R.; Phipps, D. A. *J. Chem. Soc., Dalton Trans.* **1979**, 582–595.
(33) Hamburg, A. W., Ph.D. Thesis, Purdue University, 1982.
(34) Lati, J.; Meyerstein, D. *Int. J. Radiat. Phys. Chem.* **1975**, *7*, 611–616.

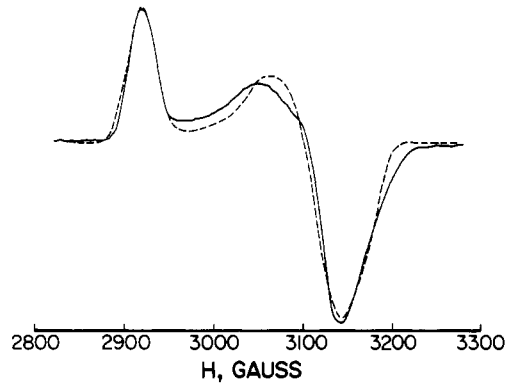

Figure 2. EPR spectrum for $Ni^{III}(H_{-1}GlyGly)_2^-$ (pH 7, 9.083 GHz, −150 °C): —, experimental; - -, calculated.

Table I. Comparison of EPR Parameters (g Values) for Nickel(III) Complexes with $g_\parallel > g_\perp$

complex	$g_\parallel$	$g_\perp$[a]	g_{av}	solvent	ref
$Ni^{III}EDTA^-$	2.34	2.14	2.21	water, pH 4.3	37
$Ni^{III}(H_{-1}GlyGly)_2^-$	2.22	2.07	2.12	water, pH 5–8	this work
$Ni^{III}(BPO)_3$	2.14	2.09	2.11	polycryst solid	38
$[Ni^{III}([12]aneN_4)]^{2+}$	2.17	2.06	2.10	acetonitrile	39
$Ni^{III}(Me_2(CH_3CO)_2$-[14]tetraenoN$_4$)]$^+$	2.14	2.07	2.09	acetonitrile	40
$Ni^{III}(TAAB)^+$	2.16	2.02	2.07	methanol	41

[a] $g_\perp$ is the average of g_{xx} and g_{yy} when resolved values were reported.

2.12) indicates that the unpaired electron is primarily at the metal center and is not a ligand radical. The spectrum has $g_\parallel > g_\perp$, in contrast to the typical situation for nickel(III) peptide complexes, where $g_\perp > g_\parallel$ for tetragonally elongated octahedral distortion. Although distinct hyperfine splitting is not observed in Figure 2, it is necessary to use hyperfine coupling constants (a_{xx}, a_{yy}, a_{zz}) as well as broadening parameters in calculations with the spectrum–matching procedure.[26] The resulting values that give the calculated spectrum in Figure 2 are $g_{xx} = 2.08$, $g_{yy} = 2.06$, $g_{zz} = 2.22$, $a_{xx} = 24$, $a_{yy} = 17$, $a_{zz} = 1$, $W_{xx} = 13.0$, $W_{yy} = 12.0$, and $W_{zz} = 15.0$. Similar EPR spectra are obtained for all the bis(dipeptide)-nickelate(III) complexes in this study.

The majority of other nickel(III) peptide complexes exhibit $g_\perp > g_\parallel$, which is best explained by a tetragonally distorted octahedral geometry with elongation of the axial bonds.[35,36] However, the situation where $g_\parallel > g_\perp$ with some other nickel(III) complexes[34–41] is summarized in Table I. In order to understand these results, the simple energy level diagram in Scheme I for d^7 nickel(III) is useful. Two of the geometries would predict $g_{zz} > g_{xx}, g_{yy}$ (i.e. $g_\parallel > g_\perp$), as shown in Table II.[42]

For a low-spin d^7 complex with a square-planar arrangement, the unpaired electron resides predominantly in the d_{xy} orbital. The predicted relationship between the g values is given in Table II, where λ is the spin–orbit coupling constant and ΔE is the energy necessary to couple the ground- and

Scheme I

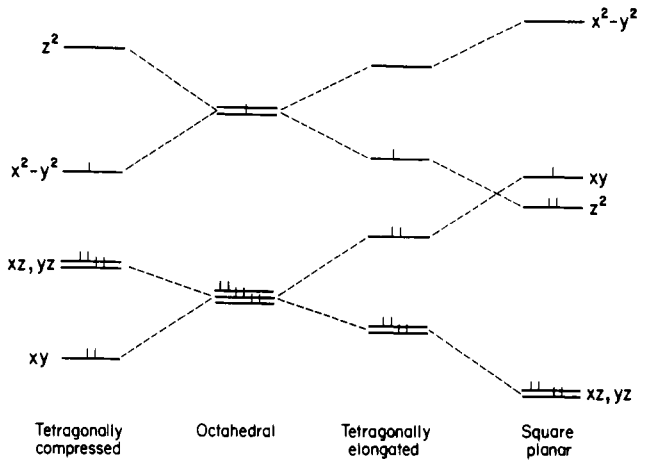

Table II. Predicted Relationship for the Relative Magnitude of EPR g Values for Tetragonally Compressed, Tetragonally Elongated, and Square-Planar Coordination Geometries for Low-Spin d^7 Nickel(III)[42]

tetragonally compressed	tetragonally elongated	square planar
$g_{xx} = 2 - \frac{2\lambda}{\Delta E_{(x^2-y^2)-yz}}$	$g_{xx} = 2 - \frac{6\lambda}{\Delta E_{z^2-yz}}$	$g_{xx} = 2 - \frac{2\lambda}{\Delta E_{xy-xz}}$
$g_{yy} = 2 - \frac{2\lambda}{\Delta E_{(x^2-y^2)-xz}}$	$g_{yy} = 2 - \frac{6\lambda}{\Delta E_{z^2-xz}}$	$g_{yy} = 2 - \frac{2\lambda}{\Delta E_{xy-yz}}$
$g_{zz} = 2 - \frac{8\lambda}{\Delta E_{(x^2-y^2)-xy}}$	$g_{zz} = 2$	$g_{zz} = 2 - \frac{8\lambda}{\Delta E_{xy-(x^2-y^2)}}$
$g_{zz} > g_{xx}, g_{yy}$ $g_\parallel > g_\perp$	$g_{xx}, g_{yy} > g_{zz}$ $g_\perp > g_\parallel$	$g_{zz} > g_{xx}, g_{yy}$ $g_\parallel > g_\perp$

excited-state energy levels for the spin-free electron. Takvoryan[41] (for $[Ni^{III}(TAAB)]^+$) and Lovecchio[40] (for $[Ni^{III}(Me_2(CH_3CO)_2[14]tetraenoN_4)]^+$) report the square-planar orientation to be the most consistent with their experimental observations.

The second arrangement that results in $g_\parallel > g_\perp$ is one in which the distortion of the octahedron is caused by compression of the axial ligand-to-metal bond lengths. For low-spin d^7 nickel(III) complexes with a compressed octahedral configuration, the unpaired electron is located primarily in the $d_{x^2-y^2}$ orbital. The EPR results of Bencini[39] for $[Ni^{III}([12]aneN_4)]^{3+}$, of Lati[37] for $Ni^{III}EDTA^-$, and of Drago[38] for $Ni^{III}(BPO)_3$ are consistent with this configuration. The EDTA and tris(BPO) ligands are hexadentate systems and prefer a distorted octahedron over the square-planar orientation. The 12-member macrocycle ([12]aneN$_4$) is too small to be square planar, must be folded to fully coordinate, and occupies two axial and two equatorial sites.[39]

In the case of the bis(dipeptide) complexes the amine nitrogens, the deprotonated peptide nitrogens, and carboxylate donors prefer a compressed octahedral environment with nickel(II)[23] and cobalt(III).[43] The crystal structures show that the distance between the two deprotonated peptide nitrogens (N^-–M–N^- axis) is 0.33 Å shorter for nickel(II)[23] and 0.15 Å shorter for cobalt(III)[43] than the amine–metal–carboxyl distance. On the basis of the crystal structure data for nickel(II) and cobalt(III) bis(dipeptide) complexes and the EPR data for the violet-black species, the proposed coordination of

(35) Nag, K.; Chakravorty, A. *Coord. Chem. Rev.* **1980**, *33*, 87–147.
(36) Haines, R. I.; McAuley, A. *Coord. Chem. Rev.* **1981**, *39*, 77–119.
(37) Lati, J.; Koresh, J.; Meyerstein, D. *Chem. Phys. Lett.* **1975**, *33*, 286–288.
(38) Drago, R. S.; Baucom, E. I. *Inorg. Chem.* **1972**, *11*, 2064–2069.
(39) Bencini, A.; Fabbrizzi, L.; Poggi, A. *Inorg. Chem.* **1981**, *20*, 2544–2549.
(40) Lovecchio, F. V.; Gore, E. S.; Busch, D. H. *J. Am. Chem. Soc.* **1974**, *96*, 3109–3118.
(41) Takvoryan, N.; Farmery, K.; Katovic, V.; Lovecchio, F. F.; Gore, E. S.; Anderson, L. B.; Busch, D. H. *J. Am. Chem. Soc.* **1974**, *96*, 731–742.
(42) Goodman, A.; Raynor, J. B. *Adv. Inorg. Chem. Radiochem.* **1970**, *13*, 135–362.
(43) Barnet, M. T.; Freeman, H. C.; Buckingham, D. A.; Hsu, I.; van der Helm, D. *J. Chem. Soc. D* **1970**, 367–368.

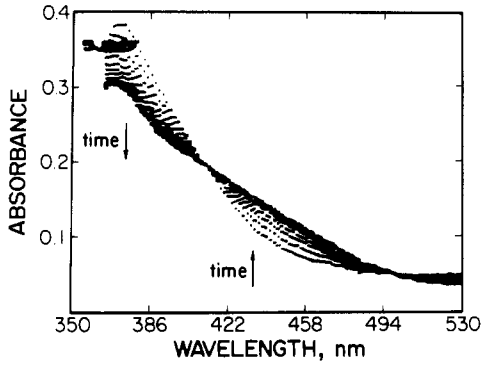

Figure 3. Vidicon spectra for the conversion of violet-black $Ni^{III}(H_{-1}GlyGly)_2^-$ to the yellow species (0.03 M $HClO_4$, 50 ms between each scan).

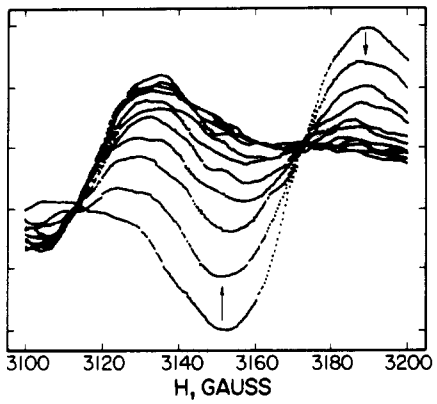

Figure 4. Aqueous (25.0 °C) EPR spectra of the conversion of violet-black $Ni^{III}(H_{-1}AlaAla)_2^-$ to the yellow nickel(III) species (0.125 M H^+, 0.35 s between scans).

the bis(dipeptide)nickelate(III) complex is given in structure **1**.

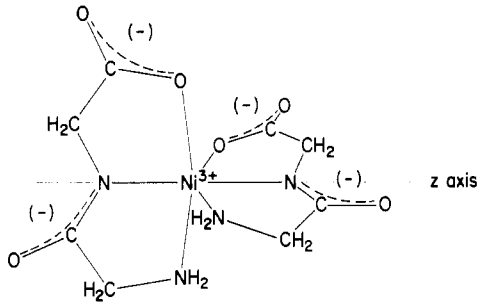

1

The proposed z axis is along the N^-–Ni^{3+}–N^- bonds. Since the unpaired electron is in the $d_{x^2-y^2}$ orbital rather than the d_{z^2} orbital, the sharp hyperfine splitting found for z-axis nitrogen donors in tetragonally elongated complexes is not observed. Sizable hyperfine coupling constants for a_{xx} and a_{yy} are found, in accord with an unpaired electron in the $d_{x^2-y^2}$ orbital. However, the broadening parameters (W_{xx}, W_{yy}) are also sizable, and therefore the hyperfine splitting is not easily observed.

The rates of disappearance of the violet-black $Ni^{III}(H_{-1}L)_2$ complexes, where L is GlyGly, AlaGly, AibGly, GlyAla, or AlaAla, have been investigated under acidic conditions. All five bis(dipeptide)nickelate(III) complexes display the same decomposition behavior, but the rates of disappearance vary with the ligand. When the violet-black complex is acidified below pH 2.3, an intensely yellow complex is formed. This reaction has been monitored with a UV–visible rapid-scanning stopped-flow spectrometer as seen in Figure 3. The presence of two isosbestic points at 409 and 500 nm indicates that there is a rapid conversion of the violet-black complex to the yellow species without the formation of appreciable intermediates. The stopped-flow rapid-scanning EPR data in Figure 4 demonstrate that the yellow species is also a nickel(III) complex.

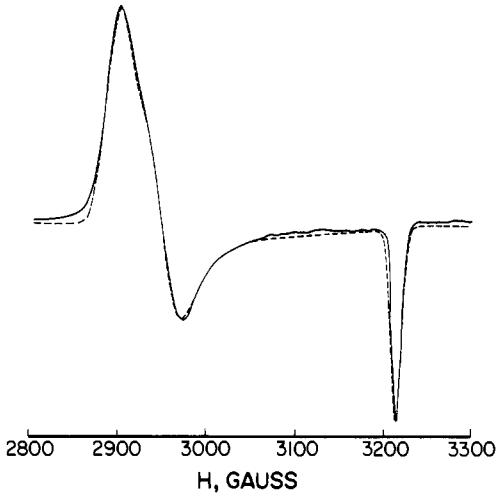

Figure 5. EPR spectrum for the yellow species generated by the acid-catalyzed rearrangement of $Ni^{III}(H_{-1}AlaGly)_2^-$ (9.080 GHz, −150 °C): —, experimental; - -, calculated.

Yellow Nickel(III) Species. The 560-nm absorption band, characteristic of the violet-black complex, disappears in the acid rearrangement. A peak at 260 nm and a shoulder at 355 nm are found, which are typical absorption bands for the yellow nickel(III) species. The conversion from the violet-black to the yellow complex is irreversible. A 0.15 mM $Ni^{III}(H_{-1}GlyGly)_2^-$ solution (pH ~7.0) was acidified (pH ~0.3, $HClO_4$) to generate the yellow complex. Within 0.1 s the mixture was neutralized (pH ~6.7) in the presence of 0.25 M excess diglycine. There was no indication of regeneration of the violet-black complex. However, the 355-nm shoulder was split into two bands at 350 and 430 nm.

In acidic media the aqueous frozen-glass EPR spectrum of the yellow species (Figure 5) is characteristic of nickel(III) complexes with a tetragonally elongated octahedral coordination ($g_\perp > g_\parallel$). The values calculated to match the spectrum in Figure 5 are $g_{xx} = 2.21$, $g_{yy} = 2.25$, $g_{zz} = 2.02$, $a_{xx} = a_{yy} = a_{zz} = 1$, $W_{xx} = 19$, $W_{yy} = 12.5$, and $W_{zz} = 6$. The g values are very similar to those for $Ni^{III}(H_{-2}DGEN)H^{2+}$ ($g_{xx} = 2.22$, $g_{yy} = 2.25$, $g_{zz} = 2.01$; DGEN is N,N'-diglycylethylenediamine).[44] This similarity suggests that four nitrogen donors (two amine and two deprotonated peptide) are still coordinated to the nickel(III). The yellow species clearly results from a rearrangement of the violet-black complex.

Decomposition Kinetics. The acid-catalyzed conversion of the violet-black complex (A) to the yellow-species (B) is followed by an acid-independent redox self-reaction to give diamagnetic products (C). The kinetic behavior can be described by a two-step sequential mechanism, eq 1, where k_1^{obsd}

$$A \xrightarrow{k_1^{obsd}} B \xrightarrow{k_2^{obsd}} C \qquad (1)$$

and k_2^{obsd} are the observed first-order rate constants. For the situation where k_1^{obsd} is larger (a factor of 5 or greater) than k_2^{obsd} and the observable species (A, B, C) have significantly different molar absorptivities, eq 2–4 can be used to deconvolute the rate constants. In eq 2–4, Y_t is the absorbance as

$$Y_t = Y_\infty - P_1 \exp(-k_1^{obsd}t) - P_2 \exp(-k_2^{obsd}t) \qquad (2)$$

$$P_1 = -[A]_0 b(\epsilon_C - \epsilon_A) - P_2 \qquad (3)$$

$$P_2 = [A]_0 b(\epsilon_C - \epsilon_B)\frac{k_1^{obsd}}{k_2^{obsd} - k_1^{obsd}} \qquad (4)$$

(44) Murray, C. K.; Margerum, D. W., unpublished results.

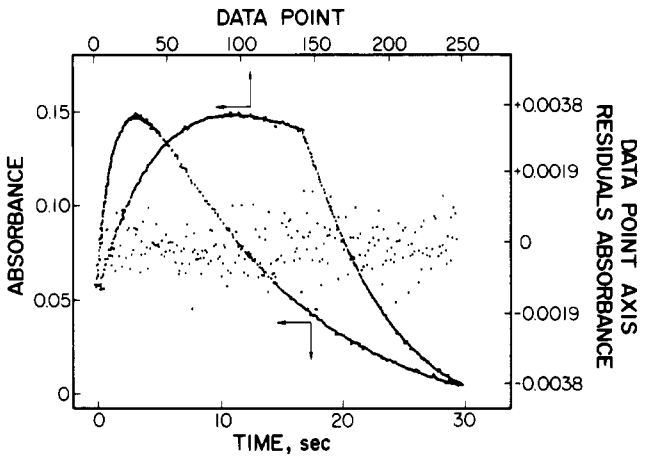

Figure 6. Absorbance as a function of time and of data points for two data acquisition rates for the reaction of $Ni^{III}(H_{-1}AibGly)_2^-$ with 0.019 M H^+ (λ_{obsd} = 450 nm). The calculated curves from eq 2–4 are superimposed and give $k_1^{calcd} = 0.48\ s^{-1}$ and $k_2^{calcd} = 0.080\ s^{-1}$. The scatter of points in the middle are the residuals from the difference between the observed and calculated absorbance values.

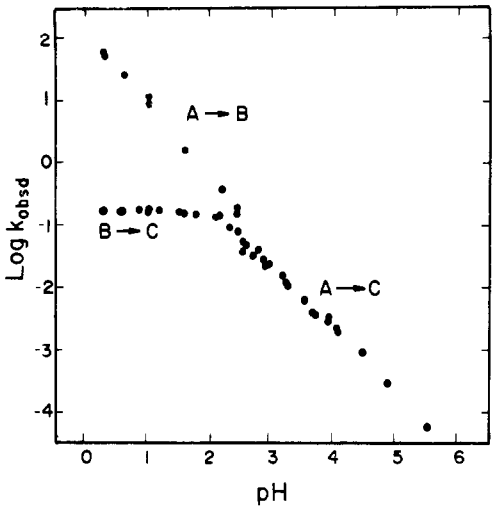

Figure 7. pH dependence of the observed rate constants for the decomposition of $Ni^{III}(H_{-1}GlyGly)_2^-$ in acidic media. Data are given in Table III.

a function of time (t), Y_∞ is the absorbance at infinite time, ϵ_A, ϵ_B, and ϵ_C are the molar absorptivities of species A, B, and C, b is the path length, and $[A]_0$ is the concentration of A at the start of the experiment. The approach developed by Ridder[45] for parallel reactions was used for data acquisition and analysis. Multiple data acquisition rates were used within each kinetic determination, so that approximately an equal number of points (ca. 125) were collected for at least the first 4 half-lives of each step.

The two-step reactions were followed at 450 nm. Figure 6 shows the absorbance change for the reaction of $Ni^{III}(H_{-1}AibGly)_2^-$ with acid (−log $[H^+]$ = 1.72). The calculated rate constants ($k_1^{obsd} = 0.48\ s^{-1}$ and $k_2^{obsd} = 0.080\ s^{-1}$) gave plots of absorbance vs. time and absorbance vs. data point that coincided with the results plotted. The residuals (the observed less the calculated absorbances) were typically small (standard deviation <0.001 or relative error <0.5%), except for the L-alanyl-L-alanine complexes where the standard deviation of residuals was slightly higher (0.005). However, this error was small (<2%) compared to the overall signal change.

Acid Dependence. Figure 7 shows the pH profile for the disappearance of $Ni^{III}(H_{-1}GlyGly)_2^-$. There are two distinct regions of differing reaction behavior. Below pH 2.3 there is a rapid acid-catalyzed conversion (A → B) of the violet-black complex to a transient intermediate (yellow species) followed by a bleaching reaction (B → C). At pH values 3–8, the violet-black complex predominates and the yellow species does not form in appreciable quantity. However, the loss of Ni(III) is catalyzed by acid. The data for these reactions are presented in Table III. Some of the reactions of $Ni^{III}(H_{-1}GlyGly)_2^-$ were followed at 409 nm, the isosbestic point for species A and B, so that k_{obsd} corresponds to the constant value k_2^{obsd} for B → C at higher acid concentrations (7.8×10^{-3} to 5.0×10^{-1} M$[H^+]$). At hydrogen concentrations below 2.8×10^{-3} M, the k_{obsd} rate constant has an acid dependence and corresponds to the k_1^{obsd} values even though B is not seen.

The rates of reaction IV the rate on the nature of the coordinating ligand. Substitution of methyl groups depend on the the first or second amino acid residue of the dipeptide affects the rate of the intramolecular rearrangement. The value of k_1^{obsd} depends upon hydrogen ion concentration (eq 5), where k_1^L is the resolved second-order rate constant for

$$k_1^{obsd} = k_1^L[H^+] \quad (5)$$

each dipeptide (L). The values for k_1^L (Table IV) were determined from the slopes of linear plots of k_1^{obsd} vs. hydrogen ion concentration. A simple linear regression model yielded a statistically zero intercept in all cases.

As seen in Table IV the rate constants for the rearrangement reaction (k_1^L) are much smaller when alanine replaces glycine in the second residue (GlyAla and AlaAla), whereas a similar replacement in the first residue leads to a somewhat larger k_1^L value. The addition of a second methyl group in the first residue (AibGly) imparts some stabilization, but not to the extent of one methyl in the second residue.

Subsequent to the rearrangement process, there is a bleaching reaction with a rate constant, k_2^L, which is independent of the acid concentration from pH 0.3–2.3. Direct monitoring of the B → C reaction is restricted to pH values less than 2.3, where an appreciable quantity of the intermediate B is formed. Above this pH the rate of formation of the yellow species is rate limiting. However, for GlyGly a small quantity of the yellow species was detected by frozen EPR up to pH 4, which suggests that the same decomposition mechanism occurs above pH 2.3. The ratio of k_1^L/k_2^L is 700 M^{-1} for GlyGly and varies from 340 M^{-1} for AlaAla to 1900 M^{-1} for AlaGly, so that separation of the A → B and B → C steps has a similar pH dependence for all the dipeptides. The disappearance of the violet-black $Ni^{III}(H_{-1}GlyGly)_2^-$ complex has a first-order dependence in hydrogen ion concentration from pH 0.3–5.5, but above pH 2.3 it is not known if this dependence is due to the peptide rearrangement reaction of nickel(III) or to the redox decomposition reaction.

In the B → C reaction, nickel(III) is reduced and part of the dipeptide is oxidized. Other studies in this laboratory of the redox decomposition of copper(III) and nickel(III) tripeptide complexes have shown that amino acid residues with methyl groups on the α-carbon tend to stabilize the trivalent oxidation state. Furthermore, the residue in the carboxyl terminal is oxidized preferentially, and the ease of this oxidation is Gly > Ala > Aib. Therefore, the reactivity sequence for k_2^L is reasonable with GlyGly > AlaGly ≅ AibGly > GlyAla > AlaAla.

Proposed Mechanism. Scheme II gives a proposed mechanism consistent with the EPR, UV–visible, and kinetics data. Proton-transfer kinetics involving metal peptide complexes have been observed to follow two pathways.[20,21] Direct peptide nitrogen protonation is general-acid catalyzed. Protonation at a peptide oxygen (outside protonation) is specific-acid catalyzed. Reactions of acid with $Ni^{II}(H_{-3}G_4)^{2-}$, $Ni^{II}(H_{-3}G_3a)^-$, $Ni^{II}(H_{-3}G_4a)^-$, and $Ni^{II}(H_{-2}GGHis)^-$ (G, Glycyl;

(45) Ridder, G. M.; Margerum, D. W. In "Essays on Analytical Chemistry"; Wanninen, E., Ed.; Pergamon Press: Oxford, 1977; pp 515–528.

Table III. Observed Rate Constants for the Reaction of Bis(dipeptide)nickelate(III) Complexes with Acid

ligand	[H⁺], M	k_1^{obsd}, s⁻¹	k_2^{obsd}, s⁻¹	ref	ligand	[H⁺], M	k_1^{obsd}, s⁻¹	k_2^{obsd}, s⁻¹	ref
GlyGly	4.8×10^{-1}	51 ± 4	0.170 ± 0.003		GlyGly	1.0×10^{-1}	11.4 ± 0.2	0.148 ± 0.001	*d*
	4.8×10^{-1}	50 ± 2	0.168 ± 0.004	*a*		9.5×10^{-2}	8.51 ± 0.06	0.165 ± 0.001	
	2.4×10^{-1}	24.7 ± 0.5	0.171 ± 0.001			2.4×10^{-2}	1.57 ± 0.01	0.149 ± 0.002	
	1.0×10^{-1}	11.6 ± 0.2	0.149 ± 0.003	*b*		6.2×10^{-3}	0.37 ± 0.002	0.145 ± 0.004	*e*
	1.0×10^{-1}	11.7 ± 0.5	0.150 ± 0.001	*c*		3.5×10^{-3}	0.181 ± 0.004	0.153 ± 0.003	*e*

ligand	[H⁺], M	k_{obsd}, s⁻¹	ligand	[H⁺], M	k_{obsd}, s⁻¹
GlyGly[f,g]	5.0×10^{-1}	0.169 ± 0.001	GlyGly[f,g]	3.1×10^{-2}	0.156 ± 0.002
	2.5×10^{-1}	0.171 ± 0.001		1.5×10^{-2}	0.140 ± 0.002
	1.26×10^{-1}	0.169 ± 0.001		7.8×10^{-3}	0.121 ± 0.002
	6.3×10^{-2}	0.166 ± 0.002			
GlyGly[g,h]	2.8×10^{-3}	$(3.63 \pm 0.03) \times 10^{-2}$	GlyGly[g,h]	2.95×10^{-4}	$(6.1 \pm 0.2) \times 10^{-3}$
	1.9×10^{-3}	$(3.1 \pm 0.2) \times 10^{-2}$		1.9×10^{-4}	$(4.0 \pm 0.2) \times 10^{-3}$
	1.2×10^{-3}	$(2.15 \pm 0.03) \times 10^{-2}$		1.2×10^{-4}	$(2.76 \pm 0.02) \times 10^{-3}$
	6.2×10^{-4}	$(1.14 \pm 0.01) \times 10^{-2}$		9.1×10^{-5}	$(2.16 \pm 0.08) \times 10^{-3}$
	8.5×10^{-5}	$(1.8 \pm 0.3) \times 10^{-3}$			
GlyGly[h,i]	4.7×10^{-3}	$(9.2 \pm 0.3) \times 10^{-2}$	GlyGly[h,i]	1.1×10^{-3}	$(2.26 \pm 0.04) \times 10^{-2}$
	2.8×10^{-3}	$(5.07 \pm 0.03) \times 10^{-2}$		6.8×10^{-4}	$(1.48 \pm 0.01) \times 10^{-2}$
	2.3×10^{-3}	$(4.8 \pm 0.1) \times 10^{-2}$		5.6×10^{-4}	$(1.11 \pm 0.02) \times 10^{-2}$
	1.6×10^{-3}	$(3.9 \pm 0.1) \times 10^{-2}$		1.2×10^{-4}	$(3.07 \pm 0.08) \times$
	1.3×10^{-3}	$(2.82 \pm 0.06) \times 10^{-2}$			
GlyGly[i,j]	2.2×10^{-4}	$(4.01 \pm 0.01) \times 10^{-3}$	GlyGly[i,j]	1.3×10^{-5}	$(3.11 \pm 0.03) \times 10^{-4}$
	3.5×10^{-5}	$(9.38 \pm 0.03) \times 10^{-4}$		3.2×10^{-6}	$(6.19 \pm 0.06) \times 10^{-5}$

ligand	[H⁺], M	k_1^{obsd}, s⁻¹	k_2^{obsd}, s⁻¹	ligand	[H⁺], M	k_1^{obsd}, s⁻¹	k_2^{obsd}, s⁻¹
AlaGly	5.0×10^{-1}	77 ± 4	0.0883 ± 0.0006	AlaGly	2.5×10^{-2}	2.04 ± 0.01	0.0851 ± 0.0003
	2.5×10^{-1}	46.0 ± 0.4	0.0864 ± 0.0003		1.2×10^{-2}	0.694 ± 0.006	0.0799 ± 0.0001
	1.2×10^{-1}	20.4 ± 0.2	0.0886 ± 0.0002		5.0×10^{-3}	0.184 ± 0.002	0.071 ± 0.01
	5.0×10^{-2}	5.91 ± 0.04	0.0872 ± 0.0008				
AibGly	4.8×10^{-1}	26 ± 1	0.081 ± 0.003	AibGly	3.8×10^{-2}	1.30 ± 0.03	0.079 ± 0.001
	2.9×10^{-1}	16.7 ± 0.2	0.0794 ± 0.0008		2.4×10^{-2}	0.69 ± 0.03	0.077 ± 0.001
	1.9×10^{-1}	9.6 ± 0.3	0.0814 ± 0.0006		1.9×10^{-2}	0.49 ± 0.01	0.078 ± 0.001
	9.5×10^{-2}	4.94 ± 0.03	0.0797 ± 0.0003				
GlyAla	4.8×10^{-1}	5.3 ± 0.4	0.034 ± 0.0004	GlyAla	3.8×10^{-2}	0.48 ± 0.02	0.0264 ± 0.0002
	2.9×10^{-1}	4.3 ± 0.5	0.0347 ± 0.0007		2.4×10^{-2}	0.29 ± 0.03	0.026 ± 0.0004
	1.9×10^{-1}	2.02 ± 0.04	0.0288 ± 0.0001		1.9×10^{-2}	0.200 ± 0.003	0.0251 ± 0.0003
	9.5×10^{-2}	1.7 ± 0.2	0.029 ± 0.003				
AlaAla	4.8×10^{-1}	2.5 ± 0.9	0.022 ± 0.001	AlaAla	1.9×10^{-2}	0.109 ± 0.005	0.0092 ± 0.0007
	1.9×10^{-1}	1.4 ± 0.4	0.016 ± 0.003				

[a] 50% Ni(III) initial concentration of previous entry. [b] 3:1 ligand to metal concentration. [c] 5:1 ligand to metal concentration. [d] 15:1 ligand to metal concentration. [e] 0.01 chloroacetic acid as a buffer. [f] I = 0.1–0.5 ($HClO_4$). [g] λ_{obsd} = 409 nm. [h] 0.01 M chloroacetic acid; I = 0.1 ($NaClO_4$). [i] 0.01 M acetic acid; I = 0.1 ($NaClO_4$). [j] λ_{obsd} = 550 nm.

Table IV. Summary of Resolved Rate Constants for the Reaction of Bis(dipeptide)nickelate(III) Complexes with Acid

dipeptide (L)	k_1^L, M^{-1} s⁻¹	k_2^L, s⁻¹	dipeptide (L)	k_1^L, M^{-1} s⁻¹	k_2^L, s⁻¹
AlaGly	160 ± 9	0.084 ± 0.006	GlyAla	12 ± 1	0.029 ± 0.004
GlyGly	105 ± 3	0.15 ± 0.01	AlaAla	5.5 ± 0.7	0.016 ± 0.006
AibGly	54 ± 2	0.079 ± 0.002			

Scheme II

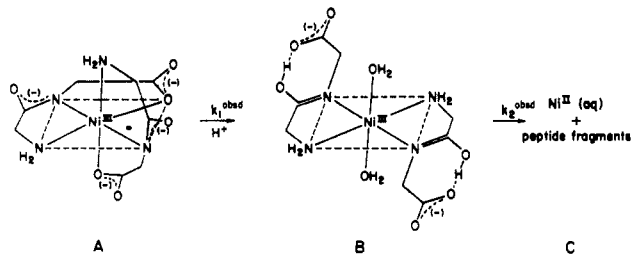

His, Histyl; a, amide) are specific-acid catalyzed.[18,46,47] Protonation of the peptide oxygen can give relatively stable species in solution. Thus, in high acid concentrations the bis(diglycine)cobaltate(III) complex forms an outside-protonated complex that has been isolated in crystalline form.[43] The crystal structure indicates that the peptide oxygen is protonated on both of the dipeptide residues. General-acid catalysis was not observed in the rearrangement of the violet-black nickel(III) complex. Therefore, we propose that the acid-induced step involves protonation of one peptide oxygen that weakens the metal to peptide bond. This promotes the rearrangement to the yellow, square-planar species. At low pH a second proton is probably added after the rate-determining step of rearrangement. The yellow species does not convert back to violet-black species in neutral solution, so the yellow species appears to be the more stable Ni(III) form even without protonation. However, the yellow species is unstable to redox decomposition and gives nickel(II). Thermal redox decomposition products of other copper(III) and nickel(III) peptide complexes show that ligand oxidations accompany reduction of the metal.[19,48-50]

Conclusion

Violet-black bis(dipeptide)nickelate(III) complexes of GlyGly, AlaGly, AlaAla, GlyAla, and AibGly have EPR spectra that are consistent with the metal in a tetragonally

(46) Paniago, E. B.; Margerum, D. W. *J. Am. Chem. Soc.* **1972**, *94*, 6704–6710.
(47) Raycheba, J. M. T.; Margerum, D. W. *Inorg. Chem.* **1980**, *19*, 497–500.
(48) Kurtz, J. L.; Burce, G. L.; Margerum, D. W. *Inorg. Chem.* **1978**, *17*, 2454–2460.
(49) Paniago, E. B.; Weatherburn, D. C.; Margerum, D. W. *J. Chem. Soc., D* **1971**, 1427–1428.
(50) Diaddario, L. L.; Farkas, J. M.; Margerum, D. W., to be submitted for publication.

compressed octahedral geometry. These complexes undergo an irreversible intramolecular rearrangement, which is acid-catalyzed, to form transient nickel(III) complexes, with EPR spectra characteristic of tetragonally elongated octahedral complexes. The rate of interconversion varies with the dipeptide in the order AlaGly > GlyGly > AibGly > GlyAla > AlaAla. The intermediate undergoes a loss of nickel(III) at a rate independent of acid concentration. Rate constants for the second step varies with the dipeptide in the order GlyGly > AlaGly ≅ AibGly > GlyAla > AlaAla.

Acknowledgment. This investigation was supported by Public Health Service Grant No. GM 12152 from the National Institute of General Medical Sciences.

Registry No. 1, 89164-56-7; bis(L-alanylglycinato)nickelate(III), 89164-57-8; bis(L-alanyl-L-alaninato)nickelate(III), 89164-58-9; bis(glycyl-L-alaninato)nickelate(III), 89164-59-0; bis(α-aminoisobutyrylglycinato)nickelate(III), 89164-60-3.

Contribution from the Dipartimento di Chimica, Università di Firenze, and ISSECC (CNR), 50132 Florence, Italy, and Dipartimento di Chimica, Università della Calabria, Calabria, Italy

Coordination Tendencies of a Series of Tetraazacycloalkanes Related to 1,4,7,10-Tetraazadecane (trien): Synthetic, Thermodynamic, and Structural Aspects

ANTONIO BIANCHI,[1a] LUCIA BOLOGNI,[1a] PAOLO DAPPORTO,[1b] MAURO MICHELONI,[1a] and PIERO PAOLETTI*[1a]

Received April 12, 1983

The macrocycle 1,4,7,10-tetraazacyclopentadecane (L5) has been synthesized. The basicity constants and the stability constants of the complexes $[ML5]^{2+}$ and $[MHL5]^{3+}$ (M = Cu(II), Ni(II)) have been determined by potentiometry at 25 °C in 0.5 mol dm^{-3} KNO_3. The enthalpies of formation of the Cu(II) and Ni(II) complexes of L5 have been determined by flow and batch microcalorimetry. The Cu(II) complex with 1,4,7,10-tetraazacyclotetradecane (L4) has been prepared and characterized by X-ray measurements. The compound $[CuL4](ClO_4)_2$ crystallizes in an orthorhombic unit cell ($P2_12_12$ space group) with lattice constants a = 22.219 (8) Å, b = 13.753 (5) Å, and c = 9.097 (4) Å, D_{calcd} = 1.66 g cm^{-3} for Z = 6, and V = 2779.8 $Å^3$. Least-squares refinement gave R = 0.076 for the 854 observed reflections. The unit cell contains two independent complex molecules. The copper atoms of both molecules are in a tetragonally distorted octahedral environment, where the four nitrogen atoms are in a planar arrangement and two oxygen atoms of two perchlorate ions in the apical positions. Among the macrocycles related to trien, L5 forms the weakest metal complexes.

Introduction

The open-chain tetraamine 1,4,7,10-tetraazadecane (trien) is one of the most familiar ligands. Many metal complexes of trien have been prepared and extensively studied both in the solid state and in aqueous solution.[2] Spectroscopic studies have shown that trien can adopt either the cis or trans configuration in octahedral complexes.[3] Beside these considerations it is also well-known that the chemistry of macrocyclic complexes has attracted considerable interest over recent years in an attempt to rationalize the special thermodynamic and kinetic properties of these complexes.[4-6] Tha aim of this work is to investigate the trends in coordination capabilities toward protons and metal ions such as Cu(II) and Ni(II) of a series of tetraazacycloalkane ligands that can be obtained by cyclization of the linear tetraamine 1,4,7,10-tetraazadecane (trien) with hydrocarbon bridges of different lengths (see structure).

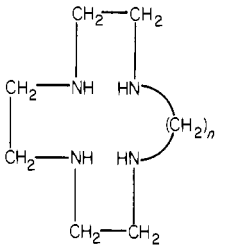

n = 0: 1,4,7,10-tetraazadecane (L1)
n = 2: 1,4,7,10-tetraazacyclododecane (L2)
n = 3: 1,4,7,10-tetraazacyclotridecane (L3)
n = 4: 1,4,7,10-tetraazacyclotetradecane (L4)

This paper reports the synthesis and the coordination properties of the macrocyclic ligand 1,4,7,10-tetraazacyclopentadecane (L5) and the crystal structure of the complex $[CuL4](ClO_4)_2$. Thermodynamic and structural data have been discussed and compared with data for the other ligands of the series, taken from the literature.

Experimental Section

Preparation of 1,4,7,10-Tetraazacyclopentadecane (L5). The tosyl derivative of L5, 1,4,7,10-tetrakis(tolyl-*p*-sulfonyl)-1,4,7,10-tetraazacyclopentadecane (I), was obtained by adding dropwise to a solution (1.3 dm^3) of the disodium salt (120 g) of *N,N',N'',N'''*-tetrakis(tolyl-*p*-sulfonyl)-1,4,7,10-tetraazadecane a solution (650 cm^3) of *O,O'*-bis(tolyl-*p*-sulfonyl)pentane-1,5-diol (53.2 g) in anhydrous DMF. The reaction mixture was refluxed for 1 h. The volume was reduced

(1) (a) Università di Firenze. (b) Università della Calabria.
(2) Basolo, F. *J. Am. Chem. Soc.* **1948**, *70*, 2634. Jonassen, H. B.; Douglas, B. E. *Ibid.* **1949**, *71*, 4094. Jacobsen, E.; Schroder, K. *J. Phys. Chem.* **1962**, *66*, 134. Marongiu, G.; Lingafelter, E. C.; Paoletti, P. *Inorg. Chem.* **1969**, *8*, 2763. Paoletti, P.; Ciampolini, M.; Vacca, A. *J. Phys. Chem.* **1963**, *67*, 1065. Wismer, R. K.; Jacobson, R. A. *Inorg. Chim. Acta* **1973**, *7*, 477. McPherson, A., Jr.; Rossmann, M. G.; Margerum, D. W.; James, M. R. *J. Coord. Chem.* **1971**, *1*, 39.
(3) Jorgensen, K. *Acta Chem. Scand.* **1957**, *11*, 399. Wilkins, R. G.; Yelin, R.; Margerum, D. W. *J. Am. Chem. Soc.* **1969**, *91*, 4326. Sacconi, L.; Paoletti, P.; Ciampolini, M. *J. Chem. Soc.* **1961**, 5115. Cook, F. D.; McKenzie, E. D. *Inorg. Chim. Acta* **1978**, *31*, 59.
(4) Izatt, R. M.; Christensen, J. J. "Synthetic Multidentate Macrocyclic Compounds"; Academic Press: New York, 1978. Melson, G. A. "Coordination Chemistry of Macrocyclic Compounds"; Plenum Press: New York, 1979. Hiraoka, M. "Crown Compounds. Their Characteristic and Applications"; Elsevier: Amsterdam, 1982.
(5) Pedersen, C. J.; Frensdorff, H. K. *Agew. Chem.* **1972**, *11*, 16. Christensen, J. J.; Eatough, D. J.; Izatt, R. M. *Chem. Rev.* **1974**, *74*, 351 and references therein. Lehn, J. M. *Acc. Chem. Res.* **1978**, *11*, 49 and references therein.
(6) Lindoy, L. F. *Chem. Soc. Rev.* **1975**, *4*, 421. Cabbiness, D. K.; Margerum, D. W. *J. Am. Chem. Soc.* **1969**, *91*, 6540. Martin, L. Y.; Dehayes, L. J.; Zompa, L. J.; Bush, D. H. *Ibid.* 1974, *96*, 4046. Kodama, M.; Kimura, E. *J. Chem. Soc., Dalton Trans.* **1976**, 116. Fabbrizzi, L.; Micheloni, M.; Paoletti, P. *Ibid.* 1980, 134. Steinmann, W.; Kaden, T. A. *Helv. Chim. Acta* **1975**, *58*, 1358.

0020-1669/84/1323-1201$01.50/0